Int. J. Heat Mass Transfer. Vol. 6, pp. 681–690. Pergamon Press 1963. Printed in Great Britain.

LAMINAR FREE CONVECTION IN CARBON DIOXIDE NEAR ITS CRITICAL POINT

H. A. SIMON and E. R. G. ECKERT

Heat Transfer Laboratory, University of Minnesota, U.S.A.

(*Received* 17 *October* 1962 *and in revised form* 14 *December* 1962)

Abstract—An experimental investigation on laminar free convection from a heated vertical flat plate immersed in carbon dioxide near its critical point is described. The test space was viewed with a Zehnder–Mach interferometer, thus giving an instantaneous picture of the distribution of refractive index. Use of the Lorenz–Lorentz equation, and equilibrium property data enabled the temperature field to be inferred, permitting the calculation of the heat-transfer coefficient and the thermal conductivity of the fluid.

Very low rates of heating were used, the temperature differences being of the order of 0·001–0·01°C, so that the constant property situation was closely approximated.

High values of the thermal conductivity and the heat-transfer coefficient were detected in the critical region, both parameters showing a dependence on the heat rate.

An engineering correlation for the heat-transfer coefficient was developed. The critical Grashof number for transition from laminar to turbulent flow was shown to be a function of the Prandtl number for the tests considered.

NOMENCLATURE

c_p, heat capacity at constant pressure;
g, gravitational constant;
Gr, Grashof number $= \dfrac{g(\rho_\infty - \rho_w)l^3\rho}{\mu^2}$;
h, heat-transfer coefficient;
k, thermal conductivity;
k_o, reference thermal conductivity = 12·7 cal/cm s degC;
K, constant in Lorenz–Lorentz equation (1);
l, distance from leading edge to point halfway up plate;
n, refractive index;
P, pressure;
Pr_o, Prandtl number $= \mu c_p/k_o$;
q, heat rate per unit area;
Ra_o, Raylcigh number $= Gr\,Pr_o$;
T, temperature;
T_c, critical temperature;
v, specific volume;
x, co-ordinate along plate;
y, co-ordinate normal to plate;
ρ, density;
ρ_c, critical density;
μ, coefficient of dynamic viscosity;
θ, angle of light to optical axis;
δ, boundary layer thickness;
L, length of heated surface.

Subscripts

c, at critical state;
o, with reference conductivity;
p, at constant pressure;
w, at wall;
∞, in fluid outside of boundary layer;
i, at first edge of heated plate encountered by light ray $X = 0$;
e, at $X = L$.

INTRODUCTION

IN RECENT years, interest has been stimulated in heat transfer occurring in a fluid near its critical state by the high heat-transfer coefficients which have been measured in this region. This makes fluids near the critical point very promising coolants for various engineering applications. Heat transfer in laminar and turbulent forced convection has been studied as well as under free convection conditions [1, 2]. The present investigation is an attempt to utilize the Zehnder–Mach interferometer for such a study.

The interferometer as a tool offers the advantage that the critical condition can be approached closer and that in particular much smaller temperature differences can be investigated than was possible in previous heat-transfer studies. On the other hand, various problems are encountered in the evaluation procedure, the most prominent being that information on thermodynamic and transport properties is required. Substances near the critical region, however, exhibit unusual phenomena which have not been adequately determined either theoretically or experimentally. Especially the behavior of their properties was found perplexing, as it appears that values obtained in various investigations are dependent on the apparatus used, on the history of handling of the fluid, and on the presence of impurities [3, 4, 5].

The present study was undertaken to examine laminar free convection on simple model configurations at temperatures slightly above the critical, and at near critical pressures [6]. The results discussed in this paper are for a vertical plate immersed in carbon dioxide. This fluid was chosen for convenience as its critical temperature, 31·04 °C, is not too different from the usual ambient temperature. Furthermore, the critical pressure, 72·85 atm,* is easily obtainable. The critical density is 0·467 g/cm³.

APPARATUS

The present paper reports on one of the geometries investigated, namely a vertical plate arranged in a cylindrical test chamber. The plate, a nichrome sheet, and the test chamber can be seen in the photograph (Fig. 1), and the test chamber itself is shown once more in Fig. 2. The chamber has an internal length of 4 in and an internal diameter of 6·5 in. Glass windows of optical quality are arranged in each of the two end plates. The windows are held in the chamber by the internal pressure only and rest on a ground plate with small elongated opening. In this way, the bending of the windows with resultant distortion of the interference fringes was kept small. Carbon dioxide was supplied from a 50 lb commercial bottle equipped with a siphon tube and is introduced into the test chamber by the tube shown on top of the chamber cylinder. The purity of the carbon dioxide in one of the bottles was checked on a mass spectrometer. Contamination by 0·07 per cent of air and

* 1 atm = 760 mm mercury column = 101325 N/m².

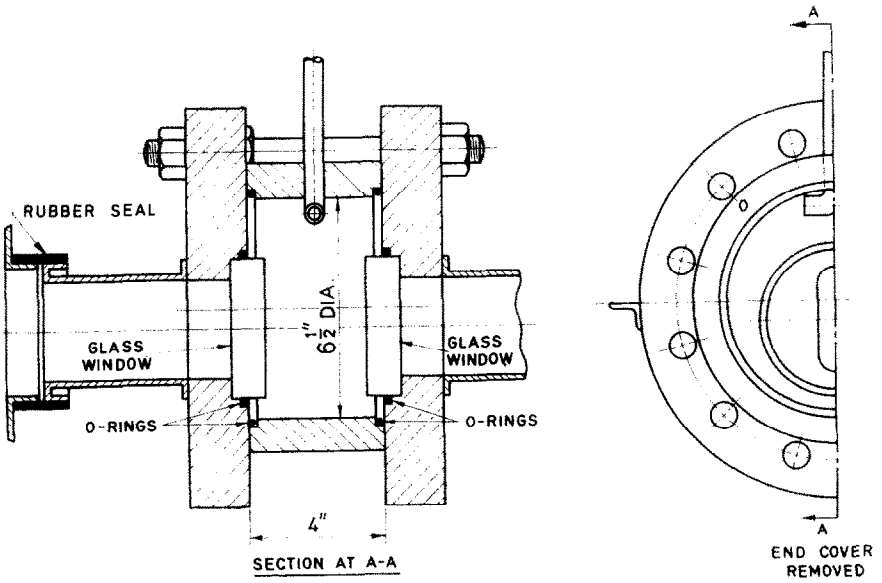

FIG. 2. Scale drawing of test chamber.

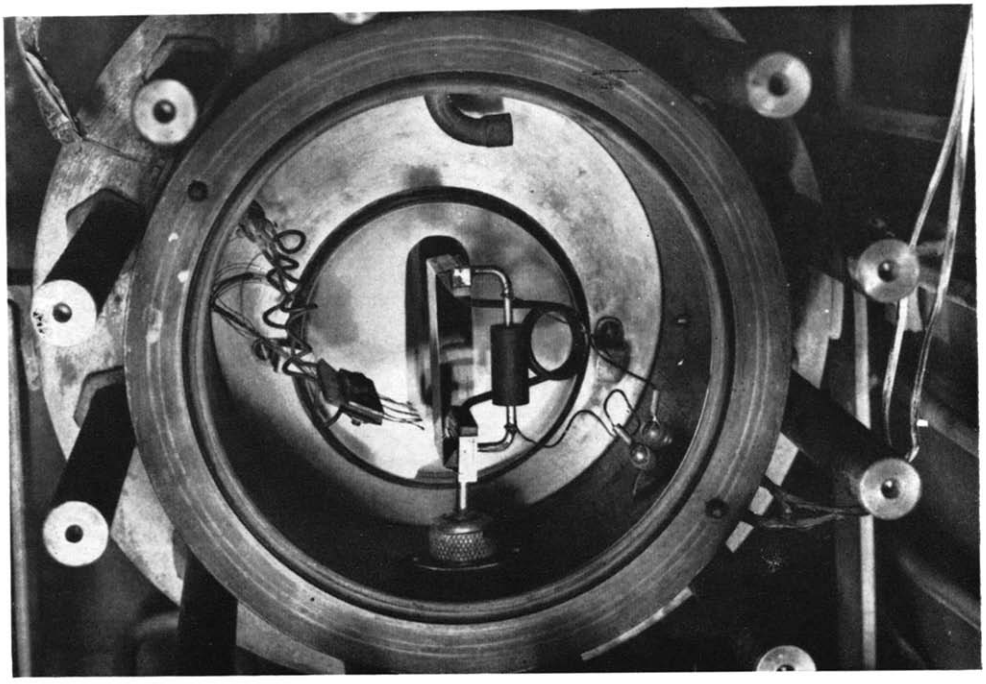

FIG. 1. Test chamber with cover removed, showing flat plate model.

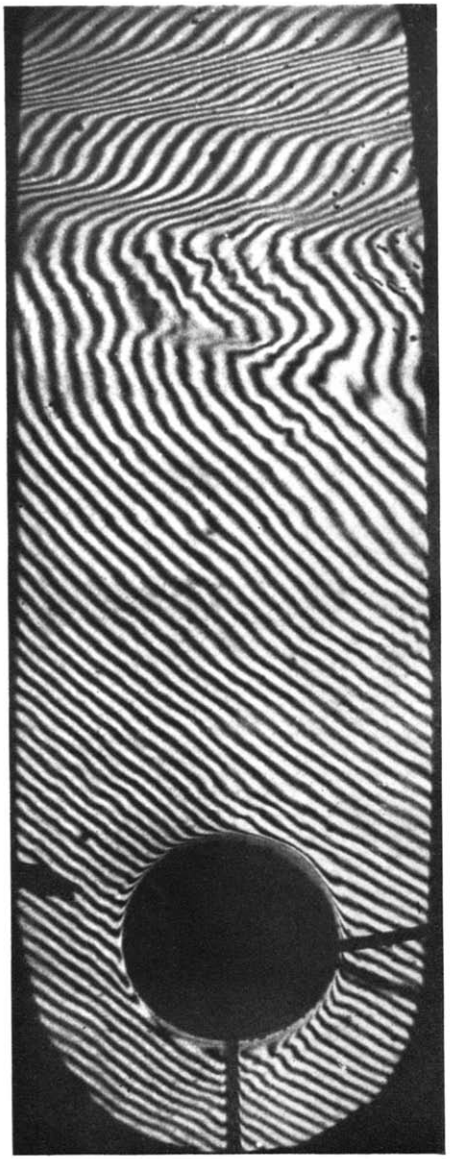

FIG. 9. Stepped gradients as occurring during heating. ($T = 34{\cdot}85°C$, $P = 77{\cdot}1$ atm, duration about 15 s.)

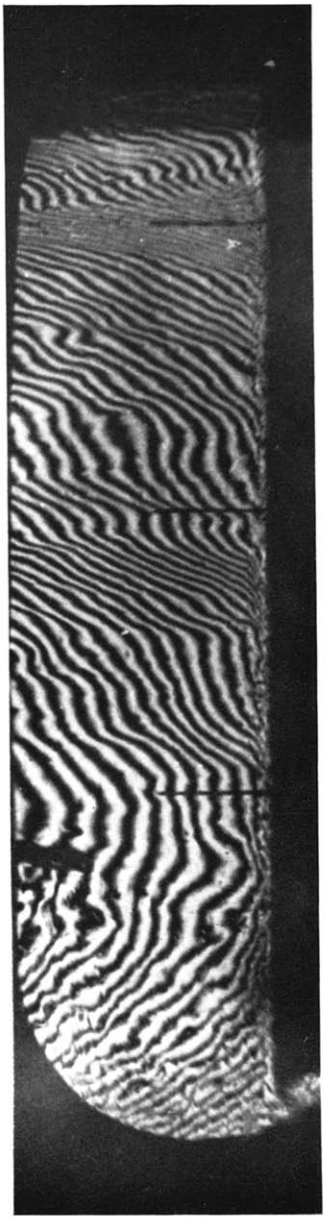

FIG. 10. Stepped gradients as occurring during establishment of equilibrium after pressure release. ($T = 32{\cdot}10°C$, $P = 74{\cdot}40$ atm, duration a few seconds.)

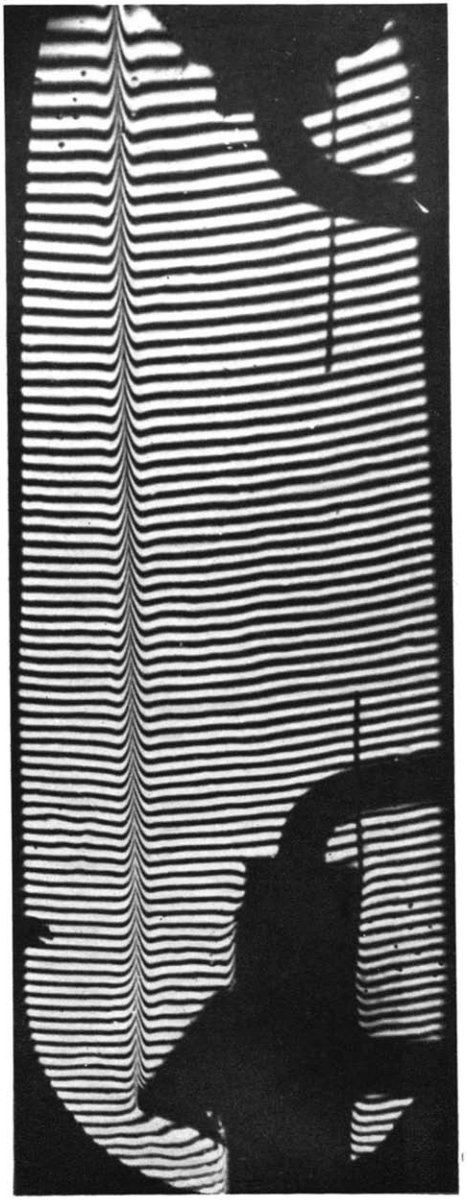

FIG. 11. Typical interferogram. ($T = 32{\cdot}14°C$, $P = 75{\cdot}49$ atm, $q = 0{\cdot}0328$ cal/h cm^2.)

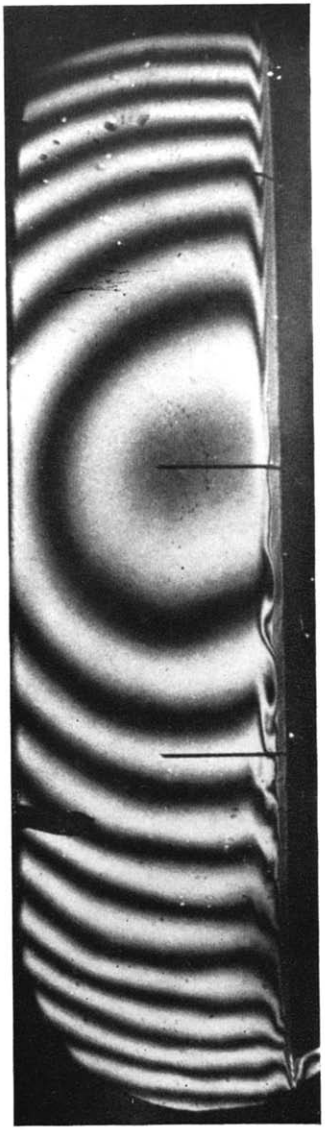

FIG. 12. Transition to turbulence. Model colder than fluid. ($T = 32{\cdot}1°C$, $P = 75{\cdot}2$ atm.)

0·08 per cent of nitrogen was measured. It is, however, possible that part of this contaminant was introduced while taking the sample.

The temperature in the working fluid was measured by five copper constantan thermocouples connected in series and arranged in a line parallel to the cylinder axis and adjacent to the model (Fig. 1). The output from the thermocouples was registered by a self-balancing potentiometer which was frequently re-calibrated against a Wenner potentiometer. The thermocouples were calibrated against a platinum resistance thermometer which in turn has been calibrated by the National Bureau of Standards with an additional check using the sodium sulfate transition point. On this basis it is estimated that the absolute temperature could be measured to 0·01 °C. Much smaller temperature differences were obtained from the interferograms.

Temperature control was achieved by immersing the entire test chamber into a thermostatically controlled water bath, the primary control coming from a Hoeppler thermostat. The stability of the temperature in the test chamber depended on fluctuations in the ambient conditions and at most underwent a slow change of about 0·03 °C in 10 min.

Pressure measurements were made with a precision dead-weight gage having an accuracy better than 0·04 per cent.

The test chamber was placed in one of the two light beams of a Zehnder–Mach interferometer. A variable width water chamber was placed in the second beam to provide adjustment for equal optical path length in both beams. The interferometer has glass plates with 6 in diameter. A detailed description of the instrument is found in [7]. The light beam traversing the test chamber did not pass through the water bath because the test chamber was connected through the tubes and rubber seals, indicated in Fig. 2, with the vertical walls of the bath.

The flat plate model was constructed from a nichrome ribbon 2·5 in long in vertical direction, 1·5 in wide in light beam direction, and 0·002 in thick, the ribbon being held taut and flat by the spring seen in Fig. 1. A storage battery provided direct current heating. The current was determined by measuring the voltage drop across an accurately determined resistance in series with the model. The measurement of the heat rate leaving the plate should not be in error by more than ± 2 per cent.

EXPERIMENTAL PROCEDURE

Prior to filling, the test chamber was flushed out with carbon dioxide from the supply bottle. It was then filled to high pressure and exhausted several times. The final filling was assisted by packing ice around the chamber and opening the supply line as rapidly as possible, thus filling the test space completely with liquid carbon dioxide. As the apparatus was not equipped with a stirrer, the fluid was first heated to several degrees above the critical temperature to avoid any persistence of the meniscus region generally associated with passage through the critical point. The test conditions were then approached, 4–6 h being required for the attainment of equilibrium. In certain cases, this equilibrium was easily maintained whereas in others, particularly near the critical point, equilibrium was a fleeting situation and only endured for a few minutes at a time. In such instances, the remaining test procedure was conducted as quickly as possible and with frequent repetitions. Even this condition could not be obtained closer than to about 1 degC to the critical point. In adjustments closer to the critical condition, circulations in the fluid as detected by the interferometer could not be avoided.

After setting the heating rate and on attainment of steady conditions, photographs were taken with the camera focused on the vertical center plane of the plate and on a plane 2–3 in distant from the first one. The second photograph was used to assist in the evaluation of the refraction error which will be discussed later on.

The state of the fluid was varied either by changing the temperature at constant density or by releasing fluid from the chamber, varying in this way the density, and then returning to the original temperature. Due to the large thermal capacity involved, the latter procedure proved to be the most convenient one.

Limitations on the rate of heating were imposed by the fluid behavior. If too low, a slow pulsating instability was evident in the

boundary layer and if too high, early transition to turbulence occurred. The temperature differences between the plate and the fluid outside the boundary layers were between 0·001 and 0·01 °C.

ANALYSIS

The evaluation of an interferogram gives directly information on the refractive index field in the fluid. This can be changed into a density distribution by use of the Lorenz–Lorentz equation.

$$\frac{n^2 - 1}{n^2 + 2} = \rho K. \qquad (1)$$

The value of the constant K for carbon dioxide was taken from [8]. It appears that this parameter exhibits no unusual behavior near the critical condition. The density difference across the boundary layer adjacent to the heated plate surface and the density gradient at the wall surface were evaluated specifically.

A number of corrections have to be made in the evaluation of an interferogram. They are well described in the literature [9]. The interferometer integrates all density variations encountered by a light ray as it travels through the working section. Near the heated surface, the light ray is bent as a consequence of the transverse density gradient. On a heated surface, as in the present investigation, the light ray is bent away from the surface. This effect gives rise to a displacement error as the plate surface appears in the photo at a location slightly different from its actual position. This shift may be determined by comparison with a photo of the unheated plate when the optical system is focused on the same plane as for the heated plate. The bending of the light beam also causes it to travel through regions of varying density. For an evaluation of this effect, the path of a light ray was calculated using Fermat's principle and assuming a parabolic density distribution within the boundary layer. The resulting difference between the density read from a local evaluation of the interferogram and the value obtained by integration along the light path can then be determined if either the emergent height at the plate end of a ray initially grazing the surface or the boundary layer thickness is known. The first value was determined with the help of a photograph taken with the camera focused on a plane 2 or 3 in from the center plane of the plate. The second value was measured from the interferogram taken with the camera focused at the center plane. The calculation of the refraction correction from both values offered a possibility to check the accuracy of this evaluation. The boundary layers become extremely thin as the critical condition is approached and, accordingly, the refraction correction may assume values of considerable magnitude. It amounted up to 25 per cent in the determination of the density difference as well as of the density gradient. It is estimated that the uncertainty in this correction causes a possible error up to ±4 per cent.

Figs. 3 and 4 present the difference between the density ρ_∞ of the fluid outside of the boundary layer and the fluid density ρ_w at the wall surface as well as the density gradient $(\partial\rho/\partial y)_w$ at the wall surface. The density ρ outside the boundary layer* is used as abscissa, and the

* The index ∞ is left off the property values where they do not appear as differences, since the variation throughout the boundary layer is negligibly small.

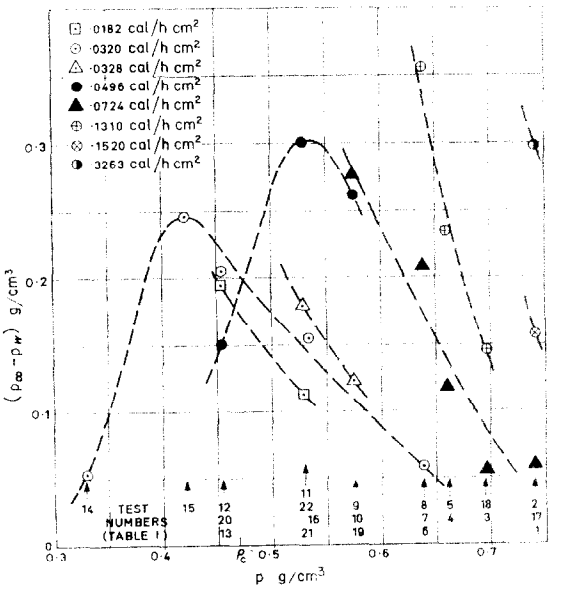

FIG. 3. Density difference across boundary layer against density in the test chamber.

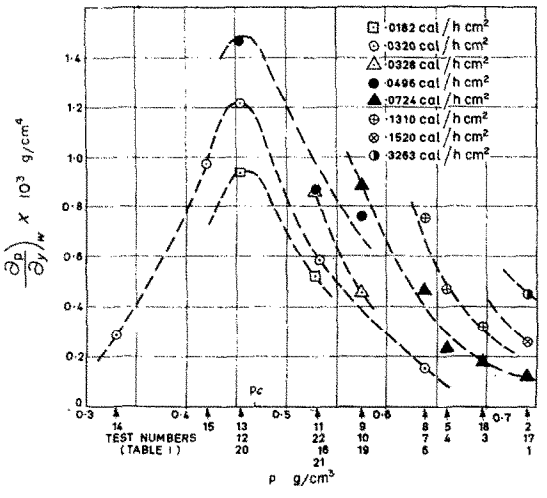

FIG. 4. Density gradient at the plate surface against density in the test chamber.

heat transferred from the plate surface into the fluid per unit time and area is kept constant on the individual curves. The test points are identified by the corresponding test numbers and Table 1 gives the corresponding test conditions. The evaluations were made at a distance from the plate leading edge halfway up the plate.

Table 1

Test No.	T_∞ (°C)	p (atm)*	ρ (g/cm³)	q (cal/h cm²)
1	30·47	88·49	0·741	0·0724
2	30·47	88·49	0·741	0·3263
3	31·60	82·37	0·696	0·0724
4	31·98	79·12	0·660	0·0724
5	31·98	79·12	0·660	0·1310
6	32·30	78·14	0·638	0·0320
7	32·30	78·14	0·638	0·0724
8	32·30	78·14	0·638	0·1310
9	32·13	75·50	0·575	0·0724
10	32·13	75·50	0·575	0·0496
11	32·12	74·91	0·528	0·0496
12	32·12	74·61	0·454	0·0320
13	32·12	74·61	0·454	0·0496
14	32·24	76·00	0·330	0·0320
15	33·65	76·84	0·421	0·0320
16	33·55	77·77	0·533	0·0320
17	30·45	88·49	0·741	0·1520
18	31·63	82·36	0·696	0·1290
19	32·14	75·49	0·575	0·0328
20	32·12	74·61	0·454	0·0182
21	32·12	74·90	0·528	0·0182
22	32·12	74·90	0·528	0·0328

* 1 atm = 101325 N/m² = 760 Torr
T_c = 31·04°C, p_c = 72·85 atm, c = 0·468 g/cm³.

Heat transfer is conventionally described by a heat-transfer coefficient obtained by dividing the heat flux q leaving the wall surface per unit area and time by an appropriate temperature potential:

$$h = \frac{q}{T_w - T_\infty}. \tag{2}$$

This then requires, in the present study, a knowledge of the temperature field, which presupposes the existence of information on the equation of state of the fluid. The results of measurements to determine the thermodynamic properties of carbon dioxide in the critical region are contained in the literature [10, 11]. However, the accent is on temperatures closer to the critical value than in the present work. Interpolation into the region of the present study was carried out graphically through the use of a pv vs. v diagram. The isotherms in such a diagram are almost straight lines. Since the temperature differences $T_w - T_\infty$ are extremely small (between 0·01 and 0·001 °C) in the present study, equation (2) could be transformed into the relation

$$h = \frac{q}{(\rho_\infty - \rho_w)\,(\partial T/\partial \rho)_p}. \tag{3}$$

The measurement of the density gradient at the plate surface made it also possible to determine the thermal conductivity appearing in Fourier's equation

$$q = -k\left(\frac{\partial T}{\partial y}\right)_w \tag{4}$$

by use of the relation (5):

$$k = -\frac{q}{\left(\frac{\partial \rho}{\partial y}\right)_w \left(\frac{\partial T}{\partial \rho}\right)_p}. \tag{5}$$

The differential quotient $(\partial T/\partial \rho)_p$ was obtained from the interpolated values of the state parameters. This again introduces a certain error, particularly near the critical condition where the isotherms are very flat. It is estimated that this error may be as large as ± 4 per cent. Even

the determination of the density in the fluid from the temperature and the pressure measurements is made difficult near the critical condition. An independent check, however, was available in that the width of the water in the compensating chamber, adjusted for maximum clarity of the fringes, was proportional to the density in the test chamber. A calibration was initially established at a temperature several degrees above the critical where the isotherm slope has conveniently large values. No remarkable deviations of the density as determined by the two methods were observed and it is estimated that the density was measured accurate to ±2 per cent in the whole range.

Figs. 5 and 6 present the heat-transfer coefficient and the thermal conductivity as determined in the way described above. From the discussion, it will have become clear that uncertainties in values presented in both figures as caused by the evaluation, increase with the approach to the critical condition. A conservative estimate of the overall errors is given in the following Table 2 for three of the test points.

It may be observed that the heat-transfer coefficient as well as the heat conductivity values peak as the critical density is approached. This is a consequence of the behavior of the parameter $(\partial T/\partial \rho)_p$ which also exhibits a large

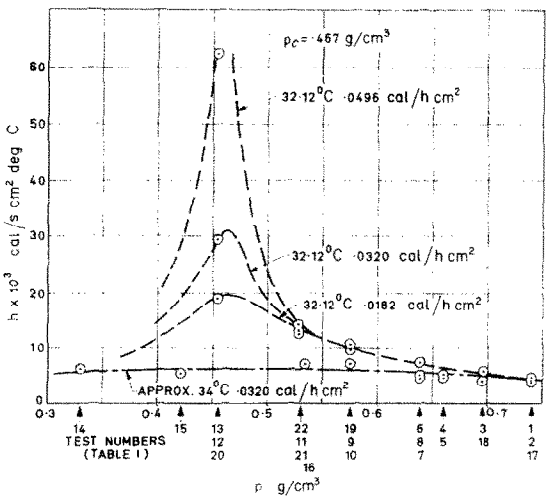

FIG. 5. Heat-transfer coefficient calculated from equation (3) against density in the test chamber.

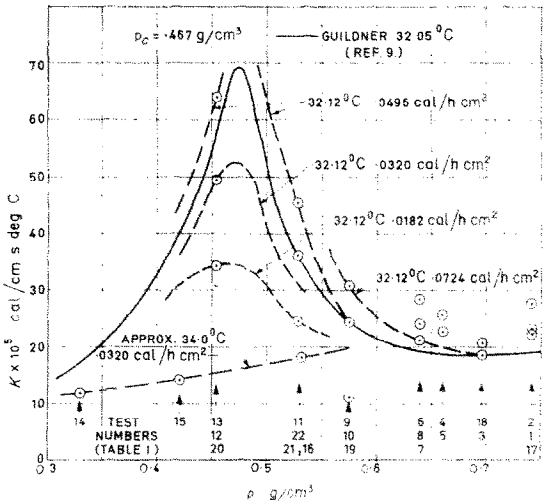

FIG. 6. Thermal conductivity of fluid calculated from equation (5) against density in the test chamber.

Table 2

Test No.	Per cent k	Per cent h
13	±20	±45
	15	25
10	15	15
3	10	6

decrease with approach to the critical state, large enough to over-compensate the increase in the density difference or in the density gradient, respectively, which, according to Figs. 3 and 4 also occurs near the critical condition. Fig. 6 exhibits a remarkable feature of the thermal conductivity. All of the dashed lines in this diagram except for the lowest one have been measured at the same temperature, 32·12°C, but at different heating rates, and it can be observed that the thermal conductivity as defined by (5) is a function of the heat rate or consequently of the local temperature gradient in addition to the state parameters density and temperature. Its value increases with increasing heat rate. Fig. 7 is a cross plot in which the thermal conductivity is presented for two density values against the heat rate q. The conductivity appears to increase approximately linearly with heat rate and extrapolation

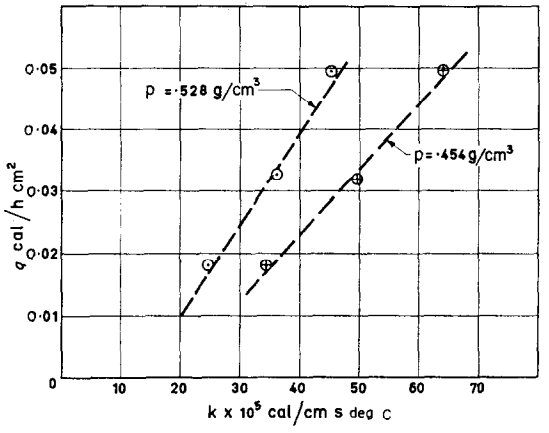

FIG. 7. Thermal conductivity against heat rate for two densities close to the critical value.

to a heat rate zero leads to values which approximately agree with the values measured at a temperature of 34·0°C and presented in Fig. 6 by the lowest dashed curve. The peculiar dependence of the heat conductivity on the heat rate appears, therefore, to be restricted to the proximity of the critical state and to disappear with decreasing heat rate. Similar observations have already been made in previous measurements of the thermal conductivity. They were usually ascribed to the occurrence of free convection currents. Such currents, however, have to be excluded in the present investigation since they would have been detected on the screen exhibiting the interferograms. The peculiar behavior of fluids near their critical condition is in the literature connected with the possibility of cluster formation. One might argue that the formation and break up of such clusters near the heated plate surface through the shear within the boundary layer is the cause of the dependence of the thermal conductivity on heat rate. Fig. 6 contains as a solid curve values for the thermal conductivity as determined by Guildner [12]. These values were again obtained from measurements at various heat rates by extrapolation to the heat rate zero. However, the measurements have been made at temperature differences which are by orders of magnitude larger than the ones used in the present investigation, and it is understandable that an extrapolation of such measurements would lead to a result different from ours. New careful measurements of the thermal conductivity of carbon dioxide near its critical pressure using small temperature gradients [16] resulted in values which appeared independent of temperature gradient and exhibited a pronounced peak near the critical point. At a temperature of 32·1°C, the values in [16] are close to those in Fig. 6 measured at a heat flow rate of 0·0182 cal/h cm². The particular behavior of the thermal conductivity raises some doubt about the justification of the conventional evaluation of heat-transfer experiments close to the critical state which is based on equilibrium thermodynamic and transport properties. Obviously more detailed studies have to be made in order to answer this question.

Various attempts have been made to find a correlation which describes for engineering purposes the heat flux as obtained in the present tests. The following relation proved most successful:

$$\frac{ql}{\rho_c k_o \left(\frac{\partial T}{\partial \rho}\right)_p} \frac{\sqrt{|T - T_c|}}{\sqrt{T_c}} = 3{\cdot}25 \times 10^{-9} \frac{Ra_o}{\sqrt{Pr_o}}. \quad (6)$$

The value 12·7 cal/cm s degC has been introduced for the thermal conductivity k_o in this equation

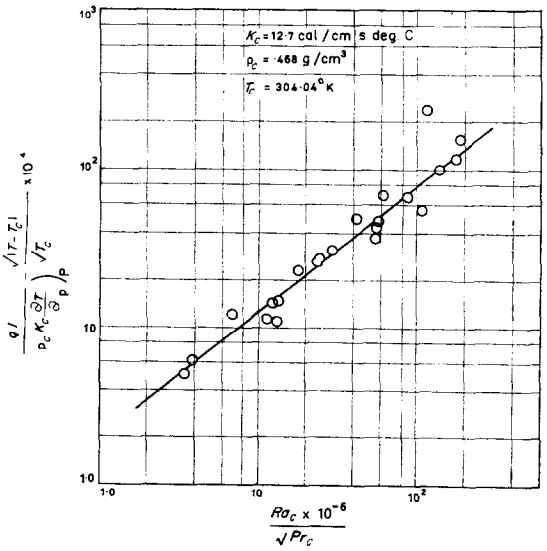

FIG. 8. Correlation of test results.

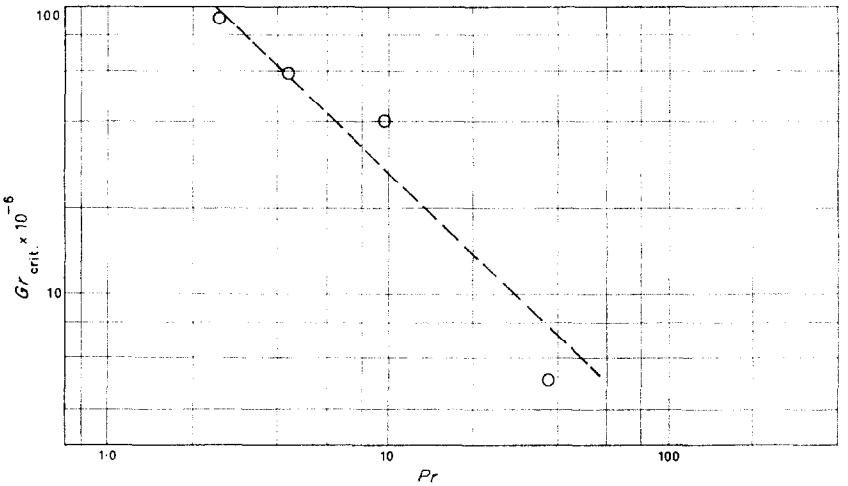

FIG. 13. Critical Grashof number for transition to turbulence against Prandtl number.

to avoid the dependance on heat flux. Values for viscosity and specific heat were taken from [13, 14, 15]. Fig. 8 indicates to what the degree experimental values agree with the equation (6) presented by the solid line.

Figs. 9–12 are reproductions of interference photos.

The peculiar behavior of the fluid near the critical state is also evidenced by the fact that occasionally stepped gradients, as shown in Figs. 9 and 10, rapidly appeared and disappeared during periods of adjustment of the test chamber conditions. These might again be connected with the formation and sedimentation of clusters. The heat-transfer models in these photos are a horizontal cylinder and a vertical plate of different construction.

It has been mentioned before that it was necessary to keep the heat rate below certain values in order to prevent transition to turbulence in the boundary layer. A few observations of the transition process have been made and the critical Grashof number for transition obtained in these is plotted against the fluid Prandtl number in Fig. 13. The critical length in the Grashof number was taken as that distance from the lower plate end at which the amplitude of the boundary layer oscillation had grown to the same order of magnitude as the boundary layer thickness. A photograph of such a transition phenomenon is shown in Fig. 12 whereas Fig. 11 represents laminar boundary layers. It is felt that the information in Fig. 13 should not be applied to other fluids without further confirmation.

On several of the interferograms, for instance in Fig. 11, a hook in the fringes is apparent at the outer edge of the boundary layer which, in the evaluation as presented before, would mean that the density goes through a maximum and the temperature of the fluid through a minimum in a region close to the outer edge of the boundary layer. No satisfactory explanation of this observation can be offered at present.

REFERENCES

1. D. L. DOUGHTY and R. M. DRAKE, JR., Free convection heat transfer from a horizontal right circular cylinder to Freon 12 near the critical state, *A.S.M.E. Trans.* **78**, 1843 (1956).
2. C. F. BONILLA and L. A. SIGEL, High intensity natural convection heat transfer near the critical point. *Fourth National Conference A.I.Ch.E.-A.S.M.E.*, Buffalo, New York (1960).
3. O. MAASS, *Chem. Rev.* **23**, 17 (1938).
4. F. D. ROSSINI, *Thermodynamics and Physics of Matter*, p. 419. Princeton University Press (1955).
5. A. MICHELS, A. BOTZEN and W. SCHUURMAN, *Physica*, **23**, 95–102 (1957).
6. H. A. SIMON, An interferometric investigation of laminar free convection in carbon dioxide near its critical point. Ph.D. Thesis, University of Minnesota (1962).
7. E. R. G. ECKERT, R. DRAKE and E. SOEHNGEN,

Manufacture of a Zehnder–Mach Interferometer. USAF Air Material Command, Dayton, Ohio, Technical Reports 5721 (1948).
8. A. MICHELS and J. HAMERS, *Physica*, **IV**, No. 10, 995 (1937).
9. R. E. BLUE, *NACA* TN 2110 (1950).
10. A. MICHELS, B. BLAISSE and C. MICHELS, *Proc. Roy. Soc.* A, 160 (1937).
11. R. H. WENTORF and C. F. BOYD, University of Wisconsin CM-724.
12. L. A. GUILDNER, *Proc. Nat. Acad. Sci.* **44**, 1149 (1958).
13. M. A. WEINBERGER and W. G. SCHNEIDER, *Canad. J. Chem.* **30**, 847 (1952).
14. A. MICHELS and S. R. DE GROOT, *Appl. Sci. Res.* A **1**, 94 (1948).
15. S. N. NALDRETT and O. MAASS, *Canad. J. Res.* **18B**, 322 (1940).
16. J. V. SENGERS and A. MICHELS, The thermal conductivity of carbon dioxide in the critical region, *Progress in International Research on Thermodynamic Properties, A.S.M.E.* (1962).

APPENDIX

Refraction error

A light ray traversing the boundary layer is refracted away from the heated surface. Thus it passes through a region of varying density near the heated surface, and passes through subsequent constant density regions at an angle to the optical axis. Errors in the indicated density field due to the latter effect are easily allowed for once the angle of the light ray is known [6, 9]. The method used to estimate the refraction error due to the light ray traversing a varying density region is indicated below.

Applying Fermat's principle to the path of a light ray, provided the angle of deflection is small, gives the following equation:

$$\frac{1}{n}\frac{\mathrm{d}n}{\mathrm{d}y} = \frac{\mathrm{d}\theta}{\mathrm{d}x}.$$

Assuming that $n \approx 1$ so that the Gladstone–Dale equation is applicable gives:

$$\frac{K}{n}\frac{\mathrm{d}\rho}{\mathrm{d}y} = \frac{\mathrm{d}\theta}{\mathrm{d}x} \quad \text{and} \quad K\frac{\mathrm{d}\rho}{\mathrm{d}y} = \frac{\mathrm{d}^2y}{\mathrm{d}x^2} \text{ for } n = 1.$$

Taking the density profile in the boundary layer to be parabolic, and given by

$$(\rho - \rho_w) = (\rho_\infty - \rho_w)(2\eta - \eta^2) \qquad (7)$$

where

$$\eta = \frac{y}{\delta} \quad \text{and} \quad \xi = \frac{x}{L}$$

one obtains

$$\frac{\mathrm{d}\rho}{\mathrm{d}\eta} = 2(\rho_\infty - \rho_w)(1 - \eta).$$

The differential equation of the light path is then

$$2(\rho_\infty - \rho_w)(1 - \eta) = \frac{\delta^2}{L^2K}\frac{\mathrm{d}^2\eta}{\mathrm{d}\xi^2}.$$

Let

$$\Omega = \frac{2L^2}{\delta^2}K(\rho_\infty - \rho_w),$$

a constant for a particular location on a steadily heated surface.

Applying the boundary conditions $\theta = 0$ at $\xi = 0$, and $\eta = \eta_e$ at $\xi = 1$ leads to the following equation for the light path:

$$\eta = \frac{(\eta_e - 1)\cos[\sqrt{(\Omega)}\xi]}{\cos\sqrt{\Omega}} + 1. \qquad (8)$$

The angle to the optical axis at which the light ray emerges from the heated surface is given by:

$$\theta_e = \frac{\delta}{L}\sqrt{(\Omega)}(1 - \eta_e)\tan\sqrt{\Omega}. \qquad (9)$$

Combining equations (7) and (8) gives ρ as a function of η and ξ.

The average density along the light path is given by

$$\rho_{AV} = \int_0^1 \rho(\xi)\,\mathrm{d}\xi, \qquad \text{for small } \theta.$$

This gives

$$\frac{\rho_{AV} - \rho}{\rho_\infty - \rho_w} = \frac{(\eta_i - 1)^2}{2}\left[1 - \frac{\sin\sqrt{(\Omega)}\cos\sqrt{\Omega}}{\sqrt{\Omega}}\right]$$

where $\eta = \eta_i$ at $\xi = 0$ and ρ is the actual density at $\xi = 0$.

For $\eta_i = 0$

$$\frac{\rho_{AV} - \rho}{\rho_\infty - \rho_w} = \tfrac{1}{2}\left[1 - \frac{\sin\sqrt{(\Omega)}\cos\sqrt{\Omega}}{\sqrt{\Omega}}\right]. \qquad (10)$$

Analysis of the interferograms including other optical corrections gives a value $(\rho_\infty - \rho_w)^+$.

Also

$$(\rho_\infty - \rho_w)^+ = (\rho_\infty - \rho_w)\left(1 - \frac{\rho_{AV} - \rho}{\rho_\infty - \rho_w}\right) \qquad (11)$$

for the light ray incident on the surface.

The above equations can now be used to estimate the refraction error if either δ or y_e are known.

Both of these parameters could be estimated from the photographs taken and in general each led to a different value of the error. This was mainly due to the fact that the density profile was not in fact parabolic, but also because neither δ nor y_e could be measured accurately. For convenience the solution was conducted graphically using both δ and y_e. The arithmetic mean of the two corrections obtained was used.

The maximum error applied was never more than about 25 per cent, and the maximum range bracketted by using δ and y_e was about ± 15 per cent of this correction or about ± 4 per cent on $(\rho_\infty - \rho_w)$.

The procedure adopted was: (i) measure δ and $(\rho_\infty - \rho_w)^1$. Use equations (11) and (12) and the equation defining Ω to determine Ω, $(\rho_\infty - \rho_w)$ and $(\rho_{Av} - \rho_w)/(\rho_\infty - \rho_w)$, (ii) measure y_e and $(\rho_\infty - \rho_w)^1$. Use equations (8) with η and $\xi = 0$, (11) and (12) and the equation defining Ω to determine δ, Ω, $(\rho_\infty - \rho_w)$ and $(\rho_{Av} - \rho)/(\rho_\infty - \rho_w)$. Finally since Ω is a constant, (10) can be used to determine the error for any η_i.

Résumé—On décrit ici une recherche expérimentale sur la convection libre laminaire à partir d'une plaque plane verticale chauffée, immergé dans du gaz carbonique au voisinage du point critique. La visualisation, faite avec un interféromètre de Zehnder–Mach, permet d'avoir une image instantanée de la distribution de l'indice de réfraction. L'utilisation de l'équation Lorenz–Lorenz et les données relatives aux propriétés d'équilibre permettent de déterminer le champ des températures et, par suite, le calcul du coefficient d'échange thermique et de la conductivité thermique du fluide.

On a utilisé des flux de chauffage très faibles, les différences de température étant de l'ordre de 0,001–0,01°C, de sorte que l'on est très près des conditions où les propriétés restent constantes.

On a trouvé, dans la zone critique, des valeurs élevées de la conductivité thermique et du coefficient d'échange, ces deux paramètres ayant une influence sur le flux de chaleur.

On a étudié une application technique du coefficient d'échange thermique. Dans les essais considérés, le nombre de Grashof critique pour la transition de l'écoulement laminaire à l'écoulement turbulent est fonction du nombre de Prandtl.

Zusammenfassung—Es wird eine experimentelle Untersuchung der laminaren freien Konvektion beschrieben an einer beheizten senkrechten ebenen Platte in Kohlendioxyd nahe dem kritischen Punkt. Der Versuchsraum wurde mit einem Zehnder–Mach-Interferometer beobachtet, was ein unmittelbares Bild der Brechungsindexverteilung lieferte. Mit Hilfe der Lorenz–Lorenz-Gleichung und den Gleichgewichtsstoffwerten erhält man das Temperaturfeld und damit den Wärme-übergangs koeffizienten und die Wärmeleitfähigkeit der Flüssigkeit.

Mit sehr kleinen Wärmestromdichten bei Temperaturdifferenzen in der Grössenordnung 0,001–0,01°C wurde der Fall konstanter Eigenschaften weitgehend angenähert.

Für die Wärmeleitfähigkeit und den Wärmeübergangskoeffizienten ergaben sich im kritischen Bereich grosse Werte, wobei beide Parameter eine Abhängigkeit von der Wärmestromdichte zeigten.

Für den Wärmeübergangskoeffizienten wurde eine Gebrauchsgleichung entwickelt. Die kritische Grashofzahl für den Übergang von laminarer in turbulente Strömungsform liess sich in den vorliegenden Versuchen als Funktion der Prandtlzahl darstellen.

Аннотация—Описывается экспериментальное исследование ламинарной свободной конвекции от нагретой вертикальной плоской пластины, погруженной в углекислоту вблизи критической точки. Наблюдения за рабочим участком производились с помощью интерферометра маха-Цендера, что давало мгновенную картину распределения значений показателя преломления. Использование уравнения Лоренца–Лоренца и данных о равновесном состоянии позволило сделать вывод относительно температурного поля, который дает возможность рассчитать коэффициенты теплообмена и теплопроводности среды.

Нагревание происходило с очень небольшими скоростями, а разность температур была порядка 0,001–0,01°C, так что в рассматриваемой области физические свойства были близки к постоянным.

В критической области наблюдались высокие значения коэффициентов теплопроводности и теплообмена, при чем обе величины находились в зависимости от скорости нагрева.

Найдена расчетная корреляция для определения коэффициента теплообмена. Показано, что в условиях опытов для переходного режима (от ламинарного к турбулентному) критическое число Грасгофа является функцией числа Прандтля.